In situ structural imaging of CO oxidation catalysis on oxidized Rh(111)

J. I. Flege and P. Sutter*
Center for Functional Nanomaterials, Brookhaven National Laboratory, Upton, New York 11973, USA
(Received 11 April 2008; revised manuscript received 12 August 2008; published 8 October 2008)

Metallic rhodium is an active catalyst for CO oxidation while the bulk Rh_2O_3 oxide is inactive, but the detailed relation between oxidation stage and reactivity is not clear at present. Here, we study CO oxidation on oxidized Rh(111) surfaces using *in situ* intensity-voltage low-energy electron microscopy. By following the structural changes during the reaction we identify the range of catalytically active surface phases between the (2×2)-O structure and the O-Rh-O trilayer corresponding to oxygen coverages between 0.25 and 2.0 ML. Further surface oxidation results in the formation of a double trilayer structure, which induces the deactivation of the catalyst.

DOI: 10.1103/PhysRevB.78.153402 PACS number(s): 82.45.Jn, 68.37.Nq, 81.65.Mq, 82.40.Np

In oxidation catalysis on metal surfaces, the formation of surface and thin-film oxides under reaction conditions has a strong influence on the activity and selectivity of the catalyst. A catalyst that is inactive in ultrahigh vacuum (UHV) can become active due to formation of oxygen-rich surface phases at high gas pressures (or vice versa): a phenomenon usually called "pressure gap." For CO oxidation catalysis on Rh it is known that its reactivity decreases under very oxygen-rich conditions. This finding has been correlated with the growth of the stoichiometric bulk oxide $Rh_2O_3(0001)$, which was concluded to poison the CO oxidation reaction.[1–3] However, the oxidation of Rh involves a number of intermediary phases,[4–6] which presumably exhibit different catalytic activities, and the question arises where along this complex oxidation pathway the "pressure gap" is actually located. In this Brief Report, we identify the range of catalytically active phases for CO oxidation on Rh(111) using spatially and temporally resolved structural fingerprinting during surface reduction in CO and oxidation in O_2.

A clean Rh(111) single-crystal surface was prepared by established procedures including repeated oxidation by O_2, high-temperature flashing, and Ar^+ ion sputtering in an UHV system. The sample was oxidized at 720 K by exposure to NO_2 at a pressure of 1×10^{-7} torr. The transformation of the surface was followed *in situ* by low-energy electron microscopy (LEEM) and low-energy electron diffraction (LEED). Following the well-known oxygen-adlayer phases at submonolayer and monolayer O coverage, further oxidation results in the formation of an O-Rh-O trilayer surface oxide,[6] which exhibits a characteristic (9×9) moiré diffraction pattern [Fig. 1(a)] and is inert to further oxidation under these conditions. Upon raising the NO_2 pressure to 1×10^{-5} torr and the sample temperature to 790 K, however, the moiré pattern slowly fades and gives way to a new pattern, which resembles a $(\sqrt{3}\times\sqrt{3})$ periodicity [Fig. 1(b)]. A time-resolved line scan analysis along the $(h0)$ direction in reciprocal space [Fig. 1(c)] indicates the emergence of a new component at about $h=0.92$ reciprocal-lattice units (r.l.u.) close to the value of 0.91 expected for the $\{11\}_{ox}$ reflections of a thin $Rh_2O_3(0001)$ film.[6] Hence, the $(\sqrt{3}\times\sqrt{3})$-like LEED pattern may also be related to the fundamental reflections of a $(1\times1)_{ox}$ unit cell of a large-cell Rhodium oxide structure and in the following we will refer to this structure as "$(1\times1)_{ox}$." LEEM shows that the surface gradually transforms from the (9×9) phase to the $(1\times1)_{ox}$ phase without noticeable formation of extended domains during the transition stage suggesting homogeneous nucleation of domains of lateral dimensions beyond the resolution limit of the microscope.

To enable the study of the individual catalytic activities and structural transformations of the (9×9) and the $(1\times1)_{ox}$ phases with respect to CO oxidation in direct comparison using intensity-voltage (I-V) LEEM,[7] distinct submicrometer-sized domains were created in the following way: First, the oxidized sample was heated at a NO_2 pressure of 1×10^{-5} torr to about 890 K, which leads to the dissolution of the $(1\times1)_{ox}$ phase in favor of an (2×1)-O adlayer in continuous areas. Subsequent cooling induced the regrowth of the (9×9) phase in these depleted regions resulting in an oxygen-rich surface with clearly separated O-Rh-O trilayer and $(1\times1)_{ox}$ domains [Fig. 2(a)]. Upon CO exposure at a temperature of 550 K, the (9×9) domains transformed from dark to bright image contrast: a signature of their gradual reduction starting at the domain boundaries,[8] while the $(1\times1)_{ox}$ phase remained unchanged. This observation indicates that the $(1\times1)_{ox}$ surface structure exhibits a higher activation barrier toward reduction in CO than the O-Rh-O trilayer domains under these reaction conditions.

To identify the structural modifications upon reduction in CO and reoxidation in O_2, we used LEEM to measure local I-V characteristics as a function of time under reaction conditions and compared the measured spectra with dynamical LEED simulations. In these experiments, we continuously acquired LEEM images over a range of energies (3–39 eV in steps of 0.4 eV) with a time step of about 80 s between each of these I-V stacks. This data set was used for structural fingerprinting of the domains marked in Fig. 2 as a function of CO and O_2 exposure. The I-V curves obtained during exposure to CO are shown in Figs. 3(a) and 3(b), respectively. While the (9×9) phase shows distinct changes with increasing CO dose, the I-V curve of the $(1\times1)_{ox}$ structure remains virtually unchanged. Subsequent exposure to O_2 at 2×10^{-7} torr induces the regrowth of the O-Rh-O trilayer structure in the reduced regions completing the catalytic cycle for CO oxidation. Thus, at this point we can already conclude that the trilayer phase delimits the range of catalytically active phases for CO oxidation on Rh(111) at 550 K

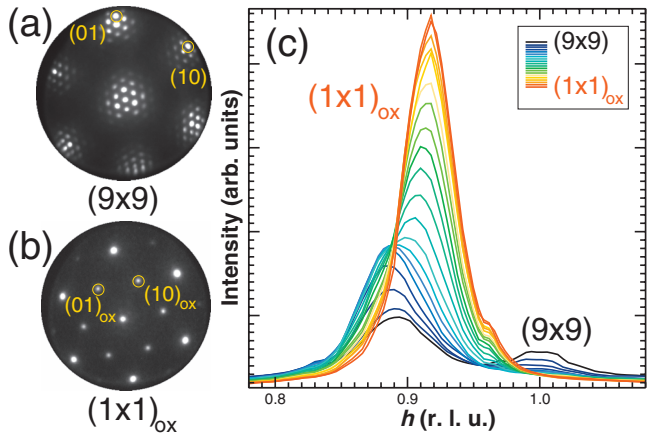

FIG. 1. (Color) (a) and (b) Low-energy electron-diffraction (E =55 eV) patterns (a) before and (b) after the phase transition occurring during oxidation of Rh(111) with NO_2 at 1×10^{-5} torr and T=790 K. (c) Time-resolved evolution of a (h0) line scan through the LEED pattern during the phase transition from the (9×9) to the $(1\times1)_{ox}$ phase.

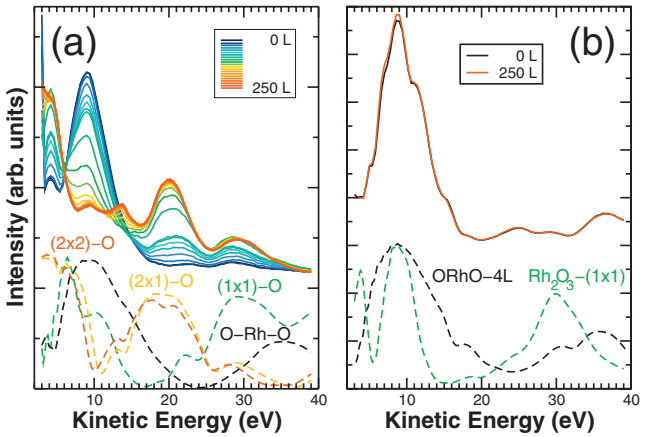

FIG. 3. (Color) Time-dependent intensity-voltage curves acquired during CO exposure at 2×10^{-8} torr (time steps 2–12) and 2×10^{-7} torr (time steps 13–26) for initially (a) (9×9)-reconstructed areas and (b) $(1\times1)_{ox}$ domains, respectively, revealing the reduction of the O-Rh-O trilayer surface to an (2×1)/(2×2)-O adlayer phase. For clarity, only every second I-V time step in the low-pressure regime is shown. Results from LEED theory are shown below for comparison (dashed lines).

and that the $(1\times1)_{ox}$ structure is already inactive. For a detailed phase identification, we performed multiple-scattering LEED calculations using the TensErLeed package[9] for DFT-calculated and experimentally determined trial structures.[6,10,11] A comparison with the experimental data clearly identifies the initial O-Rh-O trilayer, which is reduced to a (2×1)- and (2×2)-reconstructed O adlayer phase during exposure to CO. The I-V curve of the $(1\times1)_{ox}$ phase matches the simulation of a slightly stretched[12] double O-Rh-O trilayer structure[6] with a sparse Rh layer in between. This "ORhO-4L" structure has been predicted to represent an advanced oxidation state of the Rh(111) surface preceding the formation of bulklike Rh_2O_3(0001).[6] Overlaying the calculated I-V curve for this corundumlike bulk oxide phase (Fig. 3) with the experimental data, however, illustrates that this "final" stage of the surface oxidation process has not been reached yet, corroborating our experimental evidence for the existence of an additional precursor phase for Rh(111) oxidation.

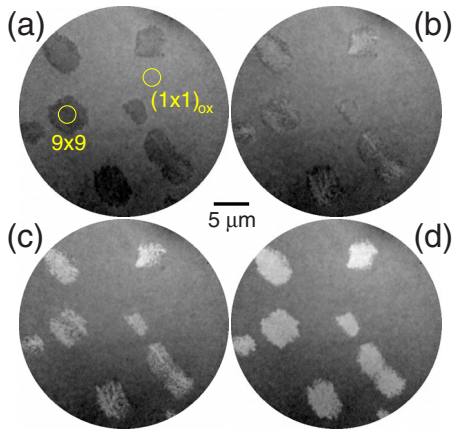

FIG. 2. (Color online) LEEM image sequence (V=4.6 eV) showing the transformation of the heterogeneously oxidized Rh(111) surface under CO exposure at 550 K. The dark patches in (a) represent the O-Rh-O trilayer regions exhibiting a local (9×9) LEED pattern; the remaining surface area is covered by the (1×1)$_{ox}$ phase. CO doses: (a) 0.0, (b) 12.1, (c) 27.3, and (d) 256.3 L.

Even for very large CO exposures (4000 L at 2×10^{-6} torr), neither the removal of the residual surface oxygen from the O-adlayer phase nor any hints of reduction in the $(1\times1)_{ox}$ structure have been observed. Hence, we can identify the catalytically active range of O coverages on Rh(111) to lie nominally between 0.25 and 2 ML, i.e., extending between the (2×2)-O and the O-Rh-O trilayer structures. Our identification of the lower limit is consistent with previous experiments on CO adsorption at room temperature, which showed the (2×2)-O overlayer to be stable for CO doses of 600 L in coexistence with a maximum CO coverage of 0.75 ML.[13]

The observed high reactivity of the O-Rh-O trilayer structure, which has very recently also been established at near-ambient pressures,[14,15] underlines the importance of subsurface oxygen species for oxidation catalysis already identified for other transition metals such as Ru (Ref. 16) and Ag (Ref. 17). In all cases, the incorporation of O atoms into subsurface sites induces a distortion of the transition-metal lattice,[18] hence decreasing the average binding energy of the surface oxygen atoms, which effectively lowers the activation barrier for the CO oxidation reaction pathway. Consequently, oxidation catalysis on Rh(111) poses a particular puzzle not found in the other transition-metal systems. The highly active O-Rh-O trilayer and the inactive ORhO-4L structures exhibit a very similar atomic bonding geometry in the near-surface region but show very different reduction rates upon CO exposure. This difference cannot be simply due to geometric differences in the CO adsorption and reaction pathway, but instead is very likely caused by other factors, e.g., defects in the trilayer[8] or its strain state. For the first effect to ultimately determine the overall reactivity of the trilayer, the individual defect densities of the O-Rh-O and the ORhO-4L structures

would need to differ by several orders of magnitude, which at least seems questionable given the fact that the thicker oxide structure grows from the trilayer, probably concomitant with a propagation of defects from the O-Rh-O seed into the upper trilayer of the ORhO-4L phase. Nevertheless, the presence of defects or the emerging O adlayer phases[8] may yet increase the reactivity. However, we note that the concept of strain-mediated activity[19] offers an alternative explanation: For the single trilayer, the observation of a (9×9) coincidence lattice in LEED gives evidence of the delicate balance struck between the energetically favorable lattice expansion due to O-O repulsion and the lack of registry of the subsurface oxygen layer to the underlying metal substrate resulting in moderate O binding energies. Conversely, the suppression of a moiré and emergence of the $(1\times1)_{ox}$ pattern for the ORhO-4L surface oxide indicates significant decoupling from the Rh metal; most likely facilitated by the sparse Rh layer separating the two O-Rh-O trilayers. Hence, albeit exhibiting basically the same near-surface geometric structure, the diminished catalytic activity could be closely connected to an effective strain release promoted by decoupling from the substrate, which leads to more strongly bound oxygen species, thereby increasing the relevant barriers for CO oxidation.

In conclusion, we have presented an *in situ* time-resolved microscopy study of the interaction of CO with oxidized Rh(111). Surface phases with oxygen coverages between 0.25 and 2 ML are highly active in CO oxidation catalysis, while adlayer structures with lower and surface oxides with higher oxygen coverage are inactive. These findings thus clearly delineate the "pressure gap" for the Rh(111) model catalyst, which is due to strong binding of surface oxygen at low coverage and is likely caused by elastic strain relaxation at the transition between an O-Rh-O trilayer surface oxide and a thicker ORhO-4L structure at high oxygen loading.

We thank P. Zahl for technical support and J. Hrbek for fruitful discussions. This work was performed under the auspices of the U.S. Department of Energy under Contract No. DE-AC02-98CH1-886.

*psutter@bnl.gov

[1] G. L. Kellogg, Phys. Rev. Lett. **54**, 82 (1985).
[2] G. L. Kellogg, J. Catal. **92**, 167 (1985).
[3] C. H. F. Peden, D. W. Goodman, D. S. Blair, P. J. Berlowitz, G. B. Fisher, and S. H. Oh, J. Phys. Chem. **92**, 1563 (1988).
[4] M. V. Ganduglia-Pirovano, M. Scheffler, A. Baraldi, S. Lizzit, G. Comelli, G. Paolucci, and R. Rosei, Phys. Rev. B **63**, 205415 (2001).
[5] M. V. Ganduglia-Pirovano, K. Reuter, and M. Scheffler, Phys. Rev. B **65**, 245426 (2002).
[6] J. Gustafson *et al.*, Phys. Rev. Lett. **92**, 126102 (2004).
[7] A. K. Schmid, W. Święch, C. S. Rastomjee, B. Rausenberger, W. Engel, E. Zeitler, and A. M. Bradshaw, Surf. Sci. **331-333**, 225 (1995).
[8] E. Lundgren *et al.*, J. Electron Spectrosc. Relat. Phenom. **144-147**, 367 (2005).
[9] V. Blum and K. Heinz, Comput. Phys. Commun. **134**, 392 (2001).
[10] S. Schwegmann, H. Over, V. D. Renzi, and G. Ertl, Surf. Sci. **375**, 91 (1997).
[11] M. V. Ganduglia-Pirovano and M. Scheffler, Phys. Rev. B **59**, 15533 (1999).
[12] The *I-V* curve shown was obtained with an increased vertical distance between the surface oxide and the Rh(111) bulk consistent with reduced coupling.
[13] J. Schoiswohl, S. Eck, M. G. Ramsey, J. N. Andersen, S. Surnev, and F. P. Netzer, Surf. Sci. **580**, 122 (2005).
[14] J. Gustafson, R. Westerström, A. Mikkelsen, X. Torrelles, O. Balmes, N. Bovet, J. N. Andersen, C. J. Baddeley, and E. Lundgren, Phys. Rev. B **78**, 045423 (2008).
[15] R. Westerström *et al.*, J. Phys.: Condens. Matter **20**, 184018 (2008).
[16] J. I. Flege, J. Hrbek, and P. Sutter, Phys. Rev. B **78**, 165407 (2008).
[17] Z. Qu, M. Cheng, W. Huang, and X. Bao, J. Catal. **229**, 446 (2005).
[18] M. Todorova, W. X. Li, M. V. Ganduglia-Pirovano, C. Stampfl, K. Reuter, and M. Scheffler, Phys. Rev. Lett. **89**, 096103 (2002).
[19] M. Mavrikakis, B. Hammer, and J. K. Nørskov, Phys. Rev. Lett. **81**, 2819 (1998).